**Modulation of the potassium channel KcsA by anionic phospholipids: Role of arginines at the non-annular lipid binding sites.**

José A. Poveda [a, 1], A. Marcela Giudici [a, 1], M. Lourdes Renart [1], Oscar Millet [2], Andrés Morales [3] and José M. González-Ros*, [1]

From [(1)] Instituto de Investigación, Desarrollo e Innovación en Biotecnología Sanitaria de Elche (IDiBE) and Instituto de Biología Molecular y Celular (IBMC), Universidad Miguel Hernández, Elche, E-03202 Alicante, Spain; [(2)] Structural Biology Unit, CICbioGUNE, Bizkaia Technology Park, Derio, 48160 Vizcaya, Spain and [(3)] Departamento de Fisiología, Genética y Microbiología, Universidad de Alicante, E-03080 Alicante, Spain.

and

Victoria Oakes [a, 4], Simone Furini [5] and Carmen Domene [4, 6, *]

From [(4)] Department of Chemistry, University of Bath, 1 South Bldg., Claverton Down, Bath BA2 7AY, The United Kingdom; [(5)] Department of Medical Biotechnologies, University of Siena, Siena, Italy and [(6)] Department of Chemistry, University of Oxford, Oxford OX1 3TA, Oxford, The United Kingdom.

[(a)] These authors contributed equally to this work

[(*)] Authors to whom correspondence should be addressed at either gonzalez.ros@umh.es or C.Domene@bath.ac.uk.

RUNNING TITLE: Ion channel modulation by anionic lipids



Formatted: English (U.S.)

KEY WORDS: Integral membrane proteins; Lipid-Protein interactions; Non-annular lipid binding sites; Ion channel inactivation; Ion channel kinetics; Patch-clamp recordings; Molecular dynamics simulations.

**List of abbreviations:**

Asolectin, L-α-Phosphatidylcholine from soybean type 2-S; DDM, dodecyl β-D-maltoside; EC1, extracellular channel loop 1; EC2, extracellular channel loop 2; HSQC, heteronuclear single quantum correlation experiment; KcsA, potassium channel from *Streptomyces lividans*; MD, molecular dynamics; PA, L-α-phosphatidic acid (egg chicken); PA4c, molecular dynamics simulation containing bound POPA to non-annular KcsA sites; PC, phosphatidylcholine; PC4c, molecular dynamics simulation containing bound POPC to non-annular KcsA sites; PG, phosphatidylglycerol; POPA, 1-Palmitoyl-2-oleoyl-sn-glycero-3-phosphatidic acid; POPC, 1-Palmitoyl-2-oleoyl-sn-glycero-3-phosphocholine; TM, transmembrane segment.

**ABSTRACT**

The role of arginines R64 and R89, present at the non-annular lipid binding sites of the KcsA potassium channel, on the modulation of channel activity by anionic lipids has been investigated. This study uses wild-type (WT) KcsA and arginine mutant channels reconstituted into membranes containing asolectin lipids and added phosphatidic acid (PA). In WT-KcsA, addition of PA drastically reduces inactivation in macroscopic current recordings. Consistent to such observations, PA causes an increase in current amplitude, mean open time and open probability at the single channel level. Moreover, kinetic analysis of single channel activity reveals that addition of PA results in longer open channel lifetimes and in a decrease in the closing rate constants. Effects akin to those of PA on WT-KcsA are observed when either one or both R64 and R89 are mutated to alanine regardless of the presence regardless of the presence of added anionic lipids. We interpret these results as a consequence of interactions between the arginines and the anionic PA bound to the non-annular sites. This receives support from NMR data which shows that at least R64 is involved in binding PA. Moreover, molecular dynamics (MD) simulations predict that R64, R89 and surrounding residues such as T61, mediate persistent binding of PA to the non-annular sites.

Channel inactivation is believed to depend on the integrity of interactions within the inactivation triad (E71-D80-W67), a group of residues behind the selectivity filter. Therefore, it is expected that such interactions become affected when PA binds the arginines at the non-annular sites. Indeed, MD simulations reveal that PA binding prevents the interaction between R89 and D80, which seems critical to keep the inactivation triad fully effective. The efficacy of this mechanism depends on the stability of the bound lipid, favoring anionic headgroups such as that of PA, which thrive on the positive charge of the arginines.

## INTRODUCTION

Membrane lipids modulate the structure and function of many integral membrane proteins and such an effect can be carried out in two different manners: i) directly, through lipid binding to specific sites on the membrane protein or ii) indirectly, by changing physical properties of the membrane bilayer. In the former, specific binding sites for lipids at transmembrane segments of the proteins are classified as annular or non-annular, depending on their lipid selectivity and binding affinity. Non-annular lipid binding sites are usually located at clefts or crevices between adjacent subunits of the membrane proteins and although there are several examples of lipid modulation through these non-annular sites (Lee, 2004; Marsh, 2008; Phillips et al., 2009; Poveda et al., 2014, 2017), the exact mechanisms through which the bound lipid exerts such a modulatory function remains elusive.

Ion channels are of the essence to many physiological and pathological processes and constitute a potentially important pharmacological target. Many studies have shown an influence of lipids on the structure and function of different ion channels and non-annular lipid binding sites have been identified as key elements in this modulation (Lee, 2004). This is the case of KcsA, a prokaryotic potassium channel that serves as a reference to the potassium ion channel superfamily due to the high homology with its eukaryotic counterparts. Anionic lipids have been shown to modulate KcsA in different manners and seem required for an optimal channel function. For instance, anionic lipids increase ion channel conductance and open probability (Iwamoto and Oiki, 2013; Marius et al., 2008), provide stability to the tetrameric channel against thermal or chemical denaturation (Raja et al., 2007; Raja, 2010; Triano et al., 2010) and enable its *in vitro* proper folding (Barrera et al., 2008), although it is still unclear how and where anionic lipids exert such effects.

From the structural view point, KcsA is a homotetramer in which the four subunits are disposed around a central pore. Each subunit contains an N-terminal cytoplasmic domain, a first transmembrane segment (TM1) connected to a pore region formed by a tilted short helix (pore helix), extracellular loops

and an ion selectivity filter, followed by a second transmembrane segment (TM2) and a final and fairly long C-terminal cytoplasmic domain (Figure 1). The selectivity filter, with the sequence TVGYG unmistakably homologous to the eukaryotic $K^+$ channels, provides a stack of ion binding sites contributed mostly by the backbone carbonyl oxygens to which potassium ions bind in a dehydrated form. Flow of ions through the pore of this channel is controlled by the opening and closing of two different gates. The inner gate is formed by a cytoplasmic bundle of helices near the C-terminal ends of each subunit. A drop in pH changes the conformation of such helical bundle, allowing the formation of an aperture that communicates the pore with the cytoplasmic solution. On the other hand, the outer gate is formed by the selectivity filter itself at the extracellular side of the protein and is stabilized in the open conformation while the inner gate is closed. However, when the inner gate opens, the extracellular outer gate becomes destabilize as to enter the inactivated conformation, where the passage of ions through the selectivity filter is impeded. This process is similar to the C-type inactivation in many eukaryotic ion channels, which also makes KcsA a good model to study this important phenomenon. A complex web of H-bonds implicating several structured water molecules and different residues behind the selectivity filter, particularly the so-called inactivation triad E71-D80-W67, have been identified as a clue element in the channel inactivation process (Bhate and McDermott, 2012; Cordero-Morales et al., 2006b, 2007, 2011; Imai et al., 2012; Ostmeyer et al., 2013; Raghuraman et al., 2014; Rotem et al., 2010).

A further examination of the KcsA crystal structure reveals that it contains non-covalently bound lipid (Zhou et al., 2001; Valiyaveetil et al., 2002) that co-crystallizes with the protein and has been identified as phosphatidylglycerol (PG) (Demmers et al., 2003). The crystallographic evidence and other studies (Deol et al., 2006) conclude that the PG binding sites in KcsA have the features of non-annular sites (Lee, 2004), i.e., a deep cleft on the protein surface, between the pore helix and TM2 of adjacent subunits. These sites bind “in vitro” other anionic phospholipids besides PG and contain two cationic arginine residues (R64 and R89) at the most extracellular side of the cleft, which are believed to be essential for binding of anionic phospholipids with high selectivity

and affinity (Deol et al., 2006; Marius et al., 2005, 2008, 2012; Weingarth et al., 2013). Moreover, it has been proposed that at least three of the four non-annular binding sites in KcsA should be occupied by anionic lipids for the channel to open (Marius et al., 2008). Additionally, these non-annular sites have been proposed to be involved in protein-protein interactions leading to the formation of KcsA clusters, which show an activity pattern very different from that of the isolated KcsA channel (Molina et al., 2015). Therefore, competing lipid-protein and protein-protein interactions involving these non-annular sites seem important factors to determine the behavior of the KcsA channel.

Besides R64 and R89 at the non-annular sites, other KcsA domains containing basic amino acid residues have been reported as sites for anionic lipid binding: i) the N-terminal R11 and K14 residues and ii) the arginine residues 27, 117, 121 and 122 located at the cytoplasmic side, close to the C-terminal segment (Figure 1). In the latter, anionic lipid binding was found to increase the stability of the channel protein against chemical denaturation (Raja et al., 2007). In the former, binding of anionic lipids reportedly induced a conformational change at the N-terminus that stabilized the open conformation of the inner gate, resulting in an increase in the open channel probability and conductance (Iwamoto and Oiki, 2013).

In this work, we have studied the role of the two arginine residues R64 and R89, present at the non-annular lipid binding sites, on the modulation of KcsA activity by anionic lipids. To do so, we have worked with wild-type KcsA and different arginine mutant channels, which have been reconstituted into asolectin lipid membranes with or without added anionic PA (phosphatidic acid). The analysis of both single-channel and macroscopic ionic currents, complemented with NMR data and molecular dynamics (MD) simulations, provides a working hypothesis in molecular terms on how lipids modulate channel inactivation.

## MATERIALS AND METHODS

Asolectin (L-α-Phosphatidylcholine from soybean type 2-S) was purchased from Sigma. PA, L-α-phosphatidic acid (egg chicken) from Avanti Polar Lipids, DDM from Calbiochem, and Bio-Beads SM-2 from Bio-Rad.

*Cloning and mutagenesis of KcsA*

The pT7-837KcsA containing the *R64A-KcsA* gene mutant was kindly donated by Professor A. Killian (Utrecht University, Holland). The R89A-KcsA mutant was obtained through site-directed mutagenesis, using the wild-type gene inserted into the pQE30 (Qiagen) plasmid as a template. The R64L and the R64,89A-KcsA double mutant were obtained using the pT7-837KcsA containing the *R64A* gene mutant as a template and the oligonucleotides 5'-ACGTATCCGCTTGCGCTGTGGTG-3' (sense) and 5'-CACCACAGCGCAAGCGGATACGT-3' (antisense) or 5´-TGACTCTGTGGGGCGCACTCGTGGCCGTGGTGGTGAT-3´ (sense) and 5´-ATCACCACCACGGCCACGAGTGCGCCCCACAGAGTCAC-3´ (antisense) (Invitrogen), respectively. All mutations were confirmed by sequencing.

*Overexpression and purification of KcsA*

Expression of the wild-type protein and the R89A mutant were performed in *Escherichia coli* M15 (pRep4) cells, whereas the R64L, R64A and R64,89A mutants were expressed in *E. coli* strain BL21(λDE3) (Molina et al., 2004). For the NMR experiments, the cells were first cultured in 5 ml of LB medium supplemented with antibiotics until an $OD_{600}$ of 0.4 was reached. This culture was diluted into 400 ml of M9 minimum medium, supplemented with thiamine, biotin and antibiotics and incubated at 37°C until an $OD_{600}$ of 0.6 was reached and finally transferred into M9 minimum medium containing 1 g/L $^{15}NH_4Cl$ (Cambridge Isotope Laboratories) to reach again a $OD_{600}$ of 0.6. In all cases, protein purification was performed essentially as previously described (Molina et al., 2004), except that the purification buffer contained 10 mM HEPES, pH 7.5, 100 mM KCl and 5 mM DDM. The higher concentration of DDM used now is aimed to reduce the formation of KcsA clusters (see below). Yields ranging 1-2

mg of purified, DDM-solubilized, tetrameric KcsA per liter of culture were routinely obtained. Protein concentrations were determined from the absorbance at 280 nm, using a molar extinction coefficient of 34,950 $M^{-1}cm^{-1}$ for the KcsA monomer (Barrera et al., 2008). The purified protein batches were also analyzed by polyacrylamide gel electrophoresis in the presence of sodium dodecyl sulfate (Molina et al., 2004).

*Reconstitution of KcsA and preparation of giant liposomes*

Wild-type KcsA and mutant channels were reconstituted in asolectin lipid vesicles, with or without an additional 25 or 50 % (by weight) of PA. In order to prepare the vesicles, the required amount of lipid was dissolved in chloroform:methanol (2:1, by volume). Then, solvents were removed using a rotary evaporator and vacuum. The dried lipid films were resuspended at 20 mg/ml in 10 mM HEPES (pH 7.0), 100 mM KCl and stored in liquid nitrogen. Before use, defrosted lipid suspensions were diluted to 5 mg/ml, then vortexed and sonicated to clarity.

To further prevent clustering of KcsA, the reconstitution step at a low lipid-protein ratio (5:1 w/w) was avoided (Molina et al., 2006, 2015). Instead, DDM-solubilized KcsA at approximately 1 mg/ml was added drop by drop to the lipid solution while being vortexed, to give a lipid to KcsA tetramer ratio of 100:1 or 1000:1 (by weight) for macroscopic or single-channel current recordings, respectively. The mixture was incubated for at least 30 minutes at room temperature. Then, the detergent was removed using Bio-Beads SM-2 (Bio-Rad laboratories) as described previously (Giudici et al., 2013). After discarding the Bio-Beads, the reconstituted KcsA liposome suspensions were collected by centrifugation (60 minutes at 300,000 x g) and finally suspended in 10 mM HEPES (pH 7.0), 100 mM KCl to a lipid concentration of 0.1 mg/µl. Samples were stored at -80 ºC.

In order to form multilamellar giant liposomes, a drop of the above reconstituted liposomes was placed on a glass slide and dried overnight in a desiccator chamber at 4ºC and then rehydrated with 20 µl of 10 mM HEPES (pH 7.0), yielding giant liposomes suitable for patch-clamp experiments after a few hours of rehydration (Riquelme et al., 1990).

*Electrophysiological recordings*

Inside-out patch clamp recordings (Hamill et al., 1981) were performed on excised patches from giant liposomes, using an automated patch clamp system (Nanion Technologies, Germany) equipped with an external perfusion device. Gigaseals were obtained on NPC-1 borosilicate glass chips (Nanion Technologies, Germany) with resistances of 3-5 MΩ. Negative pressure was applied to place a giant liposome on the aperture of the chip and form a planar lipid bilayer in the aperture (Kreir et al., 2008). After a stable seal was formed, the remaining liposomes were washed away with the corresponding intracellular buffer. Currents were recorded using an EPC-10 amplifier (HEKA Electronic, Lambrecht/Pfalzt, Germany), at a gain of 50 mV/pA. Data were digitized at a sampling rate of 10 kHz or 40 kHz (the latter only when recording +150 mV continuous pulses) and low-pass filtered to 2 or 8 kHz (Bessel filter, HEKA amplifier), respectively. Afterwards, the recordings were analyzed with Clampfit 10.3 (Molecular Devices, Axon Instruments). All measurements were taken at room temperature, with the extracellular solution containing 10 mM HEPES buffer (pH 7), 100 mM KCl and the intracellular solution 10 mM MES buffer (pH 4), 100 mM KCl.

For the recording of macroscopic currents, chips with a resistance of 2–3.5 MΩ were used. Currents were elicited in response to pH jumps from 7.0 (10 mM HEPES buffer, 100 mM KCl) to 4.0 (10 mM MES buffer, 100 mM KCl) using the perfusion system, with the membrane held at +150 mV. Maximum currents observed ranged between 250 and 2500 pA.

*Kinetic analysis*

*Preprocessing.* Kinetic analysis of single-channel recordings was done as detailed by others (Chakrapani et al., 2007a), using the QuB suite of programs (www.qub.buffalo.edu). The recordings were initially examined to eliminate those portions containing anomalous noise and overlapping channel activity. Then, they were idealized into open and close transitions using SKM, a segmental k-means algorithm based on hidden Markov modeling procedure at full bandwidth (Qin et al., 1996, 1997). Histograms of the closed and open intervals from the whole recordings, using a logarithmic abscissa and square

root ordinate (Sigworth and Sine, 1987), were fitted to a linear scheme of four closed and one open states using a maximum likelihood criteria after imposing a dead time of 25–75 μs (Chakrapani et al., 2007a).

*Isolation of Bursts.* This process was also done as in (Chakrapani et al., 2007a). Briefly, a closed-state interval longer that a critical duration ($t_{crit}$) determines when a burst of activity ends and a new one starts. Once a continuous trace is idealized and its corresponding histogram calculated and fitted to the linear scheme (see above), $t_{crit}$ was estimated as the intersection of areas between the second and third closed state durations. Isolated bursts likely arise from the activity of a single channel, which minimizes the total number of misclassified events (Jackson et al., 1983). The mean duration of open and closed times within the burst were estimated by averaging the corresponding idealized dwell times. Then, bursts were classified into low, intermediate and high mean open probability, restricting the quantitative kinetic modeling studies to the latter ones, because of their predominance and larger homogeneity. Rate constants were estimated from the dwell-time distributions of the intraburst closed and open intervals using an interval-based maximum likelihood method with an incorporated first order corrections for missed events (25–75 μs) (Ball and Sansom, 1989; Horn and Lange, 1983; Qin et al., 1996, 1997; Roux and Sauve, 1985).

*MD simulations*

The crystal structure of KcsA closed at its inner gate was retrieved from the Protein Data Bank (PDB ID 1K4C) and resolved residues 26 to 114 were used for subsequent modelling. This particular crystal structure of KcsA was chosen for this study over other available structures of the channel because it has a good atomic resolution and resembles the most the WT-KcsA channel (i.e., it has less mutations), but mainly because while having a closed inner gate at pH 7, it has a conductive selectivity filter, which makes it ideal to study its conductive to inactivated state transition. R64A, R64L and R89A mutant channels were generated using the Mutator plugin of VMD. N- and C-termini were acetylated and methylated respectively. The amino acid E71 of KcsA is modelled in the protonated state to form a diacid hydrogen bond with D80.

Default ionisation states were used for the remaining amino acids. Four water molecules were placed at the back of the selectivity filter, in agreement with crystallographic data and previous molecular dynamics (MD) simulations. SOLVATE 1.0 was used to solvate internal cavities of the protein. The structures were aligned perpendicular to the bilayer and inserted into two membrane systems: a neutral membrane containing 1-palmitoyl-2-oleoyl-sn-glycero-3-phosphocholine (POPC) and a charged membrane constituted of POPC and 1-palmitoyl-2-oleoyl phosphatidic acid (POPA) in a 3:1 ratio, with x and y dimensions of 96 Å. The VMD solvate plugin was then used to create a rectangular water box around the membrane-protein system. The overlapping water and lipid molecules around the ion channel structure were removed with the cut-off distance (1.2 Å). Potassium and chloride ions were added using Autoionize Plugin of VMD to neutralise the systems and obtain a concentration of 150 mM. The final system size was approximately 90,000 atoms.

MD simulations were performed with NAMD 2.9. CHARMM36 parameters were used for the protein and lipids, the TIP3P model was used for water, and the CHARMM NBFIX parameters for ions. The particle mesh Ewald method was used for the treatment of periodic electrostatic interactions, with an upper threshold of 1 Å for grid spacing. Electrostatic and van der Waals forces were calculated every time step. A cutoff distance of 12 Å was used for van der Waals forces. A switching distance of 10 Å was chosen to smoothly truncate the non-bonded interactions. Only atoms in a Verlet pair list with a cutoff distance of 13.5 Å (reassigned every 20 steps) were considered. The SETTLE algorithm was used to constrain all bonds involving hydrogen atoms, to allow the use of a 2 fs time step throughout the simulation. MD simulations were performed in the NPT ensemble. The Nose-Hoover-Langevin piston was employed to control the pressure with a 200 fs period, 50 fs damping constant, and the desired value of 1 atmosphere. The system was coupled to a Langevin thermostat to sustain a temperature of 300 K throughout. In the equilibration process, the same protocol was used for all of the systems. The systems were subjected to 10,000 steps of minimization, with harmonic constraints (force constant 20 kcal/mol/Å$^2$) on protein atoms, lipid headgroups and crystallographic water and ions. Harmonic restraints were gradually reduced to a force constant of 2 kcal/mol/Å$^2$

and removed in consecutive steps from the lipid headgroups, protein side-chains and protein backbone over the course of a 3.5 ns trajectory.

*NMR spectroscopy*

Two-dimensional $^{1}H,^{15}N$-HSQC (Heteronuclear Single Quantum Correlation) spectroscopy experiments were recorded on an 800 MHz Bruker Advance III spectrometer at 298 K for 5h, using detergent-solubilized $^{15}N$ isotopically enriched samples of KcsA (50 µM, tetramer) in 10 mM HEPES, pH 7.5, 100 mM KCl, 5 mM DDM. In all experiments 1024x200 points where collected and water suppression was achieved using WATERGATE. Chemical Shift Perturbation (CSP) of the arginine guanidino side chain region was used to determine the putative arginine residues from the channel that are interacting with the lipid (PA or PC) at a molar ratio of protein:lipid 1:3 (egg PA) or 1:5 (egg PC). Chemical shift perturbations were observed in the fast exchange regime and the signal corresponding to Nε-Hε of R64 was chosen as binding reporter.

## RESULTS

*Macroscopic KcsA currents*

Macroscopic WT-KcsA currents elicited by rapidly changing the pH from neutral to acidic at the intracellular side of the channel were recorded in macro patches containing a large number of KcsA channels (Figure 2). $K^+$ currents were not observed at the starting neutral pH, which is consistent with the absence of KcsA clusters from these samples (Molina et al., 2006) and suggests that the currents observed upon activation by the pH jump result from the added contributions of individual KcsA channels. Our perfusion system is not fast enough to acquire reliable data on the rapid, pH-induced channel activation, but the slower inactivation process that follows can be properly and reproducibly recorded. Figure 2A shows that KcsA reconstituted in asolectin lipids inactivates similarly to that reported by others (Chakrapani et al., 2007b), with a half-life of around one second when fitted to a single exponential and a steady-state current, $I_{ss}$ (the current remaining at the end of the pH pulse) of approximately 10% of the macroscopic peak current, $I_0$. Figure 2A also shows that addition of the anionic lipid PA to the asolectin lipid drastically reduces inactivation, leaving $I_{ss}$ values of 60% $I_0$ or higher, with no substantial differences when 25 or 50% of PA are added to the lipid matrix.

Since the non-annular sites at the extracellular side of the protein, particularly the arginines at positions 64 and 89, have been proposed as key elements for the binding of anionic lipids (see Introduction), similar experiments were conducted with arginine to alanine mutants of KcsA at such positions (R64A, R89A and the double mutant R64,89A-KcsA). Figure 2B shows that the effects on inactivation of such mutants reconstituted in plain asolectin lipids are qualitatively similar to those caused on the wild type channel by addition of PA to the membrane matrix, that is, inactivation markedly decreases in all cases. This is similar to that reported previously for the R64A mutant (Cordero-Morales et al., 2006b). Noticeably, the addition of PA to these reconstituted mutant channels has no further effects on the inactivation patterns (Figure 2C).

*Single-channel measurements*

Single-channel experiments were also performed with the WT and mutant channels from above. In these experiments, a larger lipid/protein ratio was used in the reconstitution step to disperse the channels within the bilayer and favor individual channel recordings (see Methods). In our hands, as in the early report by Schrempf's group (Meuser et al., 1999), the WT-KcsA reconstituted in asolectin lipids shows a high degree of heterogeneity in the observed potassium currents. Figure 3A is a representative example of a long recording taken at +150 mV, showing bursts of activity with different amplitudes. Such a variability is always present in different samples prepared independently or even within the same membrane patch. Figure 3B, upper panel, shows in more detail the prevailing currents from WT-KcsA reconstituted in plain asolectin lipids, which correspond to conductance values ranging 30 to 100 pS and have the common feature of exhibiting low open probabilities during the whole duration of the recordings ($NP_0 \leq 0.2$). The amplitude distribution of open states (Figure 3C, upper panel) shows that the most frequently observed current under these conditions is that of approximately 9 pA (60 pS) and its I/V plot (Figure 4) has a characteristic sigmoid-like pattern with inward and outward rectification, as reported by others (LeMasurier et al., 2001).

As to the recordings taken at negative potentials (Figure 3B, lower traces in upper panel), it is observed that channel openings are scarce, very noisy and quite heterogeneous in terms of current intensity, which is in agreement with previous reports (LeMasurier et al., 2001; Chakrapani et al., 2007a) and precluded further analysis.

Figure 3 also shows that adding PA to the reconstituted asolectin lipid bilayer has two main effects on the single-channel recordings taken at +150 mV. Figure 3B, middle and lower traces, show that although the heterogeneity in the population of currents is still maintained in presence of added PA, the predominant currents are now those with higher amplitudes. Indeed, 12 pA (80 pS) and 15 pA (100 pS) are now the most frequently observed currents in 25% and 50% added PA, respectively (Figure 3C). Such predominant currents still maintain the rectification seen in plain asolectin, regardless of the PA content

(Figure 4). Second and most noticeable, addition of PA to the reconstituted matrix, either at 25% or 50% with respect to the asolectin lipids, causes a large increase in the open probability measured during the whole duration of the recordings ($NP_0 \geq 0.8$). This has been observed previously (Iwamoto and Oiki, 2013; Marius et al., 2008; van der Cruijsen et al., 2017) and seems consistent with the marked decrease in inactivation seen in the above recordings from macro-patches. Finally, the lower traces in Figure 3B show that at negative potentials, the addition of PA to the reconstituted bilayer produces only small changes relative to the control sample in plain asolectin. The observed currents remain heterogeneous and the openings are very noisy and maintain a low open probability. At these negative potentials, the only parameter affected in a somewhat clear manner by PA addition is the intensity of the prevailing current, which is enhanced in the sample containing the highest amount of PA tested.

The KcsA arginine to alanine mutants (Figure 5) shows a much higher open probability at positive voltages compared to the single channel recordings from the WT channel, regardless of whether or not different amounts of PA were added to the asolectin lipid matrix. Again, this seems consistent with the marked decrease observed in the inactivation of these mutants (Figure 2). As in the wild-type channel, the mutants also exhibit a high degree of heterogeneity in the observed potassium currents (not shown). Figure 5 shows that the prevailing currents in these mutant channels have higher amplitudes than those of the wild-type channel in asolectin. Such an increase in current amplitudes resemble that observed when PA is added to the asolectin matrix containing the WT channel (Figure 3C). Nonetheless, in contrast to the WT channel, addition of PA to the reconstituted mutants results in little (only in the R64A-KcsA mutant) or no effects on further increasing the amplitudes of the most frequently observed currents which, additionally, show now an essentially ohmic behavior (Figure 5).

As to the observations at negative voltages in the arginine mutants, the recordings maintain a pattern similar to that of the WT channel, being essentially undistinguishable among the different mutants and remaining practically unaltered when PA was added to the reconstituted lipid matrix (Figure 5, lower traces in each panel).

*Gating kinetics*

In an attempt to further characterize the effects of PA on channel activity and the role of the arginines at the non-annular lipid binding sites in this process, an analysis of the kinetic behavior of KcsA at the single-channel level under steady-state inactivation conditions, at pH 4, was performed. Gating kinetics of WT-KcsA is highly complex and its underlying mechanisms are not yet well understood (Chakrapani et al., 2007a). There are different patterns of bursts and a large variation in the open probability and mean open and closed times from patch to path (Chakrapani et al., 2007a, 2011). Additionally, the low open probability under steady-state inactivation conditions makes it difficult to know the exact number of channels present in the patch. To partly circumvent these issues, kinetic analysis was restricted to isolated bursts, which most likely correspond to single channel activity, from the prevailing current in the continuous recordings. Moreover, such intraburst activity has been associated to conformational fluctuations at the selectivity filter (outer gate), independently of inner gate events (Chakrapani et al., 2007a), which facilitates the interpretation of the results. Finally, the analysis was confined to recordings obtained at +150 mV, both because this is the condition used in the inactivation experiments and also because at this potential the channel showed the larger open probability and the effect of lipids was more pronounced, as shown above.

The kinetic analysis of all samples follows the approach used by Chakrapani and coworkers. (Chakrapani et al., 2007a). Once the appropriate $\tau_{crit}$ (see Materials and Methods) was obtained, bursts were isolated and classified according to their intraburst open probability into low (LPo; Po<0.4), intermediate (0.4<Po<0.8) and high modes (HPo; Po>0.8). In order to study a more homogenous population, the kinetic analysis was further restricted to the open and close dwell-time histograms of HPo isolated bursts, which indeed are the most frequently observed. Relative to the distribution of closed lifetimes, Figure 6 shows that similarly to previous reports on the wild type channel in asolectin, it can be reasonably described by two components, which were assigned to a flickering and an intermediate short-lived inactivated states that KcsA would enter once it opens by acidic pH and from which the channel would recover quickly (Chakrapani et al., 2007a). Also, Figure 6 shows that the open

lifetime histogram in this case can be described by just a single component (Chakrapani et al., 2007a, 2011). When comparing these data with those from the arginine to alanine channel mutants or from the WT-KcsA channel in presence of PA, the most noticeable change detected in the histograms refers to a shift observed in the distribution of open events to longer lifetimes, which seems consistent with the slower inactivation exhibited by all these samples. To quantify these changes, the events within the bursts were fit to a kinetic model consisting of the above two closed states (the flickering and the intermediate) and one open state (Chakrapani et al., 2007a), according to:

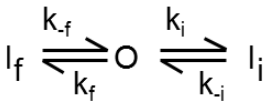

where O represents the open state, $I_f$ and $I_i$ are the inactivated flickering and intermediate states and $k_f$, $k_i$, $k_{-f}$ and $k_{-i,}$ are the corresponding closing and opening rate constants, respectively. The solid lines on top of the histograms in Figure 6 shows that such kinetic model fits reasonably well to the experimental data. Moreover, the right column in Figure 6 shows that the closing rate constants, $k_f$ and $k_{i,}$ estimated from the fits, are clearly diminished in the wild-type channel with added PA or in the arginine channel mutants relative to that of WT-KcsA in asolectin. These changes seem consistent with the observed increase in the mean open time (Figure 6, right column) and with the decrease in the rate of inactivation in those samples (Figure 2).

*Side chain charge versus size in determining the behavior of arginine mutants*

From the above results it follows that mutation to alanine of any of the two non-annular arginines strongly alters the activity pattern of KcsA and minimizes the effects of PA seen on the wild-type channel. Being a positively-charged residue, it is tempting to assume that it is the loss of such charges that determines the behavior of the arginine mutants. Nonetheless, an arginine to alanine mutation changes not only the charge, but also the size of the side chain to the much smaller alanine, which might bear on the mobility of such residue within the protein structure or on its ability to reach out for interacting

counterparts. Thus, we prepared R64L and R89L-KcsA mutants, since the leucine side chain is also non-charged, but larger than that of alanine. Unfortunately, only the R64L mutant could be expressed as a tetrameric channel protein in our expression system and therefore, the experiments that followed were done only with this latter channel. Figure 7A shows that in sharp contrast to the arginine to alanine mutants, the R64L mutant inactivates quite rapidly as evidenced in macro-patch recordings, in a manner practically undistinguishable to that seen in the WT channel. Moreover, addition of PA to the asolectin lipid matrix does not modify appreciably the observed inactivation rate. Single-channel experiments also show that the R64L mutant has an activity pattern similar to that of WT-KcsA (Figure 7B), i.e., characterized by a low open probability. Moreover, kinetic analysis of the R64L mutant channel, also included in Figure 6 to facilitate comparison, yields short opening times and high closing rate constants, essentially identical to those of the WT channel. It should be emphasized that R89 is still present in the R64L mutant and therefore, all the effects reported for this mutant are due to the substitution by leucine of just a single arginine residue.

*NMR measurements of phospholipid binding*

The interaction between PA and the KcsA channel was further investigated using NMR spectroscopy in detergent-solubilized samples. NMR is a suitable technique to determine intermolecular interactions with atomic resolution and a $^{15}$N-labeled sample of KcsA was used to monitor the NHε moiety of the guanidino group of the arginine side chains, whose chemical shift is located in a fairly clean region of the $^{1}$H,$^{15}$N-HSQC (Figure 8). Actually, this region is quite crowded in this particular protein, consistent with the abundant Arg residues that belong to the KcsA channel. The two terminal R189 and R190 are more flexible and they are tentatively assigned to the most intense signals of the spectrum, while R89 and R64 are unequivocally assigned after recording the $^{1}$H,$^{15}$N-HSQC spectra of the R89A- and R64A-KcsA mutant channels. Addition of PC does not cause noticeable chemical shifts of any of the spectral signals. On the contrary, the presence of added PA results in significant chemical shifts affecting arginine side chains. Remarkably, R64 shifts about 0.5 ppm in the $^{15}$N dimension, reflecting a change in the chemical environment of the residue as a

consequence of interaction with the added anionic phospholipid. A direct interaction between the lipid and the side-chain is the most straightforward explanation and is in line with the MD simulations below. Due to signal overlap, R89 cannot be equally monitored.

*Structural basis of lipid modulation of KcsA inactivation*

As mentioned in the Introduction, the KcsA selectivity filter is comprised of four ion-binding sites, formed by a tetrameric arrangement of backbone carbonyl atoms of residues T75 to G79, in addition to the side-chain of T75, and an external site. The canonical conformation of the filter is stabilized by H-bonding with surrounding amino acids, mainly those at the W67-E71-D80 inactivation triad (Cordero-Morales et al., 2011). Residues Y78 (selectivity filter) and D80 (pore loop) H-bond with residue E71 (pore helix), whilst D80 also H-bonds with W67 (pore helix). Structured water molecules also contribute to the structural integrity of this region (Ostmeyer et al., 2013; Weingarth et al., 2014). In view of its critical role on inactivation, our attention~~s~~ ~~are~~ is focused toward~~s~~ the behavior of this triad region in order to understand the initial steps of the inactivation process and how membrane lipids may be involved.

MD simulations of KcsA (PDB 1K4C) were performed in zwitterionic (PC) and mixed zwitterionic/anionic (PC/PA) lipid bilayers. At the outset, simulations were initiated from a random lipid configuration (see Methods), denoted $^{n}$WT-PA or $^{n}$WT-PC where n indicates the replica. Over the course of these simulations, performed in duplicate, both zwitterionic and anionic lipid molecules were observed to occupy non-annular binding sites on the interface between two adjacent subunits. The cleft is lined with hydrophobic residues from TM1 (L40), the pore helix (P63, L66 and W67) and TM2 (L86, C90 and V93), with the lipid headgroup capable of interacting with charged and polar residues in the immediate locale (T61, R64 and R89). The observed site is in agreement with those previously postulated (Deol et al., 2006; Marius et al., 2012) and with regions of electron density assigned as bound anionic lipid molecules in crystal structures of KcsA (Valiyaveetil et al., 2002). On account of this, additional simulations were performed with lipids bound into the four identical non-annular lipid binding sites, denoted $^{n}$WT-PA$_4$ or $^{n}$WT-PC$_4$, where n indicates the replica.

The binding pose used for each lipid was extracted from the most highly populated cluster observed in the replica 1 of the corresponding random lipid simulation ($^{1}$Wt-PA or $^{1}$Wt-PC) and docked into each site. A summary of all the simulations performed can be found in Table 1.

Striking differences in the inactivation triad environment are observed on comparison of the WT channel when lipids are present at the non-annular sites, relative to when they are absent (Figure 9). In the second replica of the simulation of wild type KcsA in the PA membrane, $^{2}$WT-PA, where the lipid is just randomly distributed around the protein, persistent H-bonds are formed between non-annular arginine R89, and triad residue D80 for between ~40-80% of the simulation in all tetramer subunits (Figure 9A). In contrast, in the WT-$PA_4$ simulations, where the lipid is bound to the non-annular sites, the equivalent interaction frequency reaches only a maximum of ~20% in all subunits (Figures 9A and S1). This can be attributed to preferred H-bonding between R89 and the negatively charged headgroup of PA bound to the adjacent site. Bound PA typically exhibits a stable and persistent binding pose in which an ester oxygen atom at the apex of an acyl chain H-bonds to R89, whilst the phosphate oxygen atoms of the headgroup H-bond to R64 (Figure 9C). The frequency of these H-bonds is generally in excess of 80% in at least three non-annular sites. Moreover, phosphate oxygen atoms are also capable of simultaneously H-bonding T61, and the T61-PA H-bond frequencies are observed to be between 50-60% (Table S1). Overall, each non-annular PA is involved in approximately 2.5 H-bonds at one time (Figures 9B and S1). In contrast, the H-bond frequencies between the zwitterionic PC and the equivalent protein residues are highly variable (T61 0-80%, R64 40-90% and R89 30-90%; Table S1). In two out of five WT-$PC_4$ replicas, the proposed D80-R89 interaction is predominant in one or two subunits (H-bond frequency > 50%). In the remaining three replicas, this interaction is reduced in all subunits (H-bond frequency < 20%; Figures 9 and S1). Representative examples of both scenarios are shown in Figures 9C and D. The increased D80-R89 interaction observed in the PC simulations appear to correlate with diminished H-bonding with this lipid. It is therefore more probable that the D80-R89 interaction will form when the non-annular lipid species is PC rather than PA. In this respect, it should also be

taken into account that the non-annular sites have been shown experimentally to have a higher selectivity for binding anionic over zwitterionic lipids (Marius et al., 2005, 2008). Therefore, it is likely that some of these sites would not be occupied when in the presence of just zwitterionic phospholipids, thus, further favoring the D80-R89 interaction.

Because of the involvement of R64 and R89 in the above processes, an equivalent simulation protocol was utilized for KcsA arginine mutants (Figure 10A). In the R64 mutants, lower D80-R89 H-bond frequencies (averaged over all subunits) are reported for all R64A-KcsA simulations (PA, $PA_4$, PC and $PC_4$), relative to the corresponding R64L-KcsA simulations. This seems consistent with our experimental findings on the different inactivation exhibited by these two mutants. These differential effects can be ascribed to the bulkiness of the leucine sidechain, which induces a shift in R89 towards D80 shown in Figure 10B. On the other hand, the R89A-KcsA mutant presents a very different, alternative scenario. In this case, the removal of the arginine destabilizes the conformation of W67, resulting in its detachment from D80. This movement coincides with the breakage of the E71-D80 H-bond, culminating in complete disruption of the inactivation triad in two to four subunits (Table 2). This suggests that R89 is important to reinforce the conformation of the inactivation triad and maintain its stability. Such effect is observed irrespectively in neutral and anionic lipid bilayers, with and without bound non-annular lipids, with an average percentage of disrupted states over all four subunits between 35 and 80%. This dramatic effect on the inactivation triad seen in the R89A mutant, however, is not observed in any of the other simulations (Table 2). In all other cases, the average percentage of disrupted states over all four subunits ranges only between 0 and 15%.

## DISCUSSION

This work aims to shed further light on the modulation of KcsA function by anionic lipids and to decipher the role on such process of arginines R64 and R89 present at the non-annular lipid binding sites. Our results show that addition of the anionic lipid PA to the asolectin lipid matrix containing the reconstituted KcsA drastically changes the behavior of the WT channel at the single-channel level, causing a slowdown of the closing rates and consequently, an increase in the mean open time and the open probability. Such alterations would be expected to result in a marked decrease in channel inactivation, as it is indeed observed experimentally by macroscopic current measurements in presence of added PA.

Effects akin to those of PA on the WT channel are observed when either one or the two arginines are mutated to alanine. Studies using the single arginine to alanine mutants (R64A or R89A-KcsA) show that the resulting arginine/alanine combinations are not enough to resemble the inactivation pattern of the WT channel. In stark contrast with this, the arginine to leucine R64L mutant shows that the bulkier leucine side chain, although uncharged, could substitute R64 in maintaining the inactivation features of the wild-type channel. This suggests that the interactions leading to alteration of channel inactivation features by the arginines are to some extent non-electrostatic in nature. It should also be emphasized that, in spite of their different behavior, neither the arginine to alanine mutants, nor the R64L mutant show additional alterations in inactivation when in the presence of added anionic phospholipids. Therefore, it should be concluded that both arginine residues are needed to mediate the effects caused by the presence of PA on KcsA function.

In line with previous postulates referred in the Introduction (Zhou et al., 2001; Valiyaveetil et al., 2002; Triano et al., 2010; Deol et al., 2006; Weingarth et al., 2013), we interpret our electrophysiological results on the WT channel as a consequence of interactions between the arginines and anionic lipids bound to the non-annular sites. This receives support from the NMR data which strongly suggests that at least R64 is specifically involved in binding the anionic

PA, although the experimental system used for the NMR experiments consisted just of detergent-solubilized protein and added lipid. Moreover, our MD simulations predict that R64, R89 and surrounding residues such as T61, are involved in persistent binding of the anionic phospholipid head group to the non-annular sites. Since channel inactivation is considered under control by the inactivation triad, it is expected that the specific binding of anionic phospholipids, should affect the inactivation triad in some manner, either directly or indirectly. This notion is supported by evidence that the mutation of residues constituting the triad (Cordero-Morales et al., 2011, 2006b) results in a slowdown of the inactivation process, similar to that reported here when anionic lipids are present or when the arginines are mutated to alanine. Our MD simulations suggest that non-annular anionic lipids are pivotal to the inhibition of direct D80-R89 interactions. Moreover, our simulations of the R64A and R64L mutants bolster opposing effects on D80-R89 interactions, in keeping with the divergent inactivation of these mutants, as reported in this study. With this in mind, we advocate that the behaviour of the inactivation triad, and hence the inactivation process, may be modulated by direct attachment of R89 to D80. The interaction between PA at the non-annular site and R89, as well as the R64A mutation, prevents this interaction, and both factors are associated with diminished inactivation, supporting this idea. In the simulations of the R89A mutant, the lack of R89 results in full disruption of the inactivation triad, which might explain why inactivation in this mutant in particular, no longer occurs. Such disruption, however, is not observed in simulations of any other non-inactivating experimental condition. Considering the simulation results presented, it can be suggested that, rather than disruption, subtler effects resulting from the detachment of R89 to the inactivation triad, via D80, are taking place, which lead also to the partial loss of the ability to inactivate.

Since the arginines at the non-annular lipid binding sites appear as relevant sites for the functional modulation of KcsA by anionic phospholipids, it should be taken into account that there are four equivalent, non-annular lipid binding sites per channel and a pertinent question would be, how many sites need to be occupied by the bound lipids to exert their effects on the inactivation rate? Previous proposals suggest that occupation of at least three equivalent non-

annular sites is necessary for channel opening (Marius et al., 2008), although the differences in experimental conditions makes difficult the extrapolation to our system. Furthermore, coarse-grained simulations observed minimal binding affinity to a single site when the remaining three sites are occupied, suggesting occupation of three sites is optimum (Weingarth et al., 2013). We observed saturation of the lipid effects on inactivation at 25% of PA added to the asolectin matrix, but the asolectin lipids themselves already contain an approximately 10% of different anionic lipids (McCormick and Johnstone, 1988), plus those retained bound at the non-annular sites of KcsA upon its purification. In our simulated bilayers for the MD study, the four non-annular sites in each channel remain lipid-bound during the time course of the simulation. However, it is possible that on extended timescales, expulsion of phospholipid molecules from some of such sites could take place. Indeed, although speculative, our simulation results insinuate that full occupancy of non-annular sites may not be required, considering that the zwitterionic PC is also capable of perturbing the D80-R89 interaction, albeit to a lesser extent.

The overall conclusion is that the inactivation properties of KcsA are influenced by the interaction between the inactivation triad residues and the non-annular arginines. The presence of phospholipids bound at the non-annular sites, particularly anionic ones, prevents such interactions, providing a potential explanation in molecular terms on how lipids modulate channel inactivation. In the MD simulations, the anionic PA binds securely to the non-annular sites, as a result of persistent H-bonding with T61, R64 and R89, inhibiting the D80-R89 interaction; in contrast, the H-bonding attributes of zwitterionic lipids (PC) are more variable, and thus the interactions between the arginines and the inactivation triad are more likely to be established. Functionally, these predictions seem consistent with the diminished inactivation observed experimentally when the concentration of anionic lipid is increased in the bilayer containing the WT channel. It should be noted, however, that this proposal is based on the comparison between electrophysiological observations made at an acidic pH and at a positive holding potential, with data from KcsA crystals and from our own MD simulations, which are obtained at neutral pH and in the absence of any electrical gradient. This could be an important limitation to our

interpretations and in fact, single channel recordings at negative voltages from both the wild-type channel and arginine to alanine mutants, in the presence of added PA, are similar to those from wild-type channel in plain asolectin, i.e. very few and short apertures, consistent with the maintenance of “WT-like” inactivation under these hyperpolarizing conditions. Nonetheless, such a departure from our interpretation can be rationalized by considering that at hyperpolarizing potentials the E71-D80 interaction is enhanced, as a result of the voltage-dependent orientation of the E71 residue (Cordero-Morales et al., 2006a). Therefore, it seems that an adequate E71-D80 interaction, which becomes stronger at negative voltages, is a main determinant of inactivation. In fact, the only reported case in which inactivation at negative voltages can be removed is that of the E71A mutant (Cordero-Morales et al., 2006a).

The prokaryotic KcsA is often considered a simplified version of eukaryotic potassium channels and therefore, we search for similarities at putative non-annular lipid binding sites in different eukaryotic channels. An equivalent to R89 is conserved in many $K^+$ channels (mostly as either an arginine or a lysine), but that equivalent to R64 is conserved only in a few instances, such as the human Kv5.1 channel, where a glutamine residue is found at that position (McCoy and Nimigean, 2012). Thus, it is conceivable that some eukaryotic potassium channels should be able to bind anionic phospholipids to these sites and behave similarly to KcsA in terms of its functional modulation by lipids.

**ACKNOWLEDGEMENTS**

This work was partly supported by grants BFU2012-31359 and BFU2015-66612-P from the Spanish MINECO/FEDER, UE and by BBSRC and Pfizer (BB/L015269/1) through a studentship to V. Oakes. We acknowledge PRACE for awarding us access to computational resources in ARCHER the UK National Supercomputing Service (http://www.archer.ac.uk), the PDC Centre for High Performance Computing (PDC-HPC), CINECA in Italy, and Jülich Supercomputing Centre in Germany. Likewise, we acknowledge RES (Red Española de Supercomputación) for providing resources at Picasso in the University of Malaga, one of the nodes of RES. Mrs. Eva Martinez provided excellent technical help throughout this work.

## REFERENCES


Ball, F.G., and M.S. Sansom. 1989. Ion-channel gating mechanisms: model identification and parameter estimation from single channel recordings. *Proc.r.soc.l. B Biol.Sci.* 236:385–416.

Barrera, F.N., M.L. Renart, J.A. Poveda, B. De Kruijff, J.A. Killian, and J.M. González-Ros. 2008. Protein self-assembly and lipid binding in the folding of the potassium channel KcsA. *Biochemistry*. 47:2123–2133.

Bhate, M.P., and A.E. McDermott. 2012. Protonation state of E71 in KcsA and its role for channel collapse and inactivation. *Proc.Natl.Acad.Sci.U.S.A*. 109:15265–15270.

Chakrapani, S., J.F. Cordero-Morales, V. Jogini, A.C. Pan, D.M. Cortes, B. Roux, and E. Perozo. 2011. On the structural basis of modal gating behavior in K(+) channels. *Nat.Struct.Mol.Biol.* 18:67–74.

Chakrapani, S., J.F. Cordero-Morales, and E. Perozo. 2007a. A quantitative description of KcsA gating II: single-channel currents. *J.Gen.Physiol*. 130:479–496.

Chakrapani, S., J.F. Cordero-Morales, and E. Perozo. 2007b. A quantitative description of KcsA gating I: macroscopic currents. *J.Gen.Physiol*. 130:465–478.

Cordero-Morales, J.F., L.G. Cuello, and E. Perozo. 2006a. Voltage-dependent gating at the KcsA selectivity filter. *Nat.Struct.Mol.Biol.* 13:319–322.

Cordero-Morales, J.F., L.G. Cuello, Y. Zhao, V. Jogini, D.M. Cortes, B. Roux, and E. Perozo. 2006b. Molecular determinants of gating at the potassium-channel selectivity filter. *Nat.Struct.Mol.Biol.* 13:311–318.

Cordero-Morales, J.F., V. Jogini, S. Chakrapani, and E. Perozo. 2011. A multipoint hydrogen-bond network underlying KcsA C-type inactivation. *Biophys.J.* 100:2387–2393.

Cordero-Morales, J.F., V. Jogini, A. Lewis, V. Vasquez, D.M. Cortes, B. Roux, and E. Perozo. 2007. Molecular driving forces determining potassium


Formatted: English (U.S.)

Formatted: English (U.S.)

channel slow inactivation. *Nat.Struct.Mol.Biol.* 14:1062–1069.

van der Cruijsen, E.A.W., A. V. Prokofyev, O. Pongs, and M. Baldus. 2017. Probing Conformational Changes during the Gating Cycle of a Potassium Channel in Lipid Bilayers. *Biophys. J.* 112:99–108. doi:10.1016/j.bpj.2016.12.001.

Demmers, J.A., D.A. van, K.B. de, A.J. Heck, and J.A. Killian. 2003. Interaction of the K+ channel KcsA with membrane phospholipids as studied by ESI mass spectrometry. *FEBS Lett.* 541:28–32.

Deol, S.S., C. Domene, P.J. Bond, and M.S. Sansom. 2006. Anionic phospholipid interactions with the potassium channel KcsA: simulation studies. *Biophys.J.* 90:822–830.

Giudici, A.M., M.L. Molina, J.L. Ayala, E. Montoya, M.L. Renart, A.M. Fernández, J.A. Encinar, A. V. Ferrer-Montiel, J.A. Poveda, and J.M. González-Ros. 2013. Detergent-labile, supramolecular assemblies of KcsA: Relative abundance and interactions involved. *Biochim. Biophys. Acta - Biomembr.* 1828:193–200.

Hamill, O.P., A. Marty, E. Neher, B. Sakmann, and F.J. Sigworth. 1981. Improved patch-clamp techniques for high-resolution current recording from cells and cell-free membrane patches. *Pflügers Arch. Eur. J. Physiol.* 391:85–100. doi:10.1007/BF00656997.

Horn, R., and K. Lange. 1983. Estimating kinetic constants from single channel data. *Biophys.J.* 43:207–223.

Imai, S., M. Osawa, K. Mita, S. Toyonaga, A. Machiyama, T. Ueda, K. Takeuchi, S. Oiki, and I. Shimada. 2012. Functional equilibrium of the KcsA structure revealed by NMR. *J.Biol.Chem.* 287:39634–39641.

Iwamoto, M., and S. Oiki. 2013. Amphipathic antenna of an inward rectifier K+ channel responds to changes in the inner membrane leaflet. *Proc.Natl.Acad.Sci.U.S.A*. 110:749–754.

Jackson, M.B., B.S. Wong, C.E. Morris, H. Lecar, and C.N. Christian. 1983.

Successive openings of the same acetylcholine receptor channel are correlated in open time. *Biophys.J.* 42:109–114.

Kreir, M., C. Farre, M. Beckler, M. George, and N. Fertig. 2008. Rapid screening of membrane protein activity: electrophysiological analysis of OmpF reconstituted in proteoliposomes. *Lab Chip*. 8:587. doi:10.1039/b713982a.

Lee, A.G. 2004. How lipids affect the activities of integral membrane proteins. *Biochim.Biophys.Acta*. 1666:62–87.

LeMasurier, M., L. Heginbotham, and C. Miller. 2001. KcsA: it's a potassium channel. *J.Gen.Physiol*. 118:303–314.

Marius, P., S.J. Alvis, J.M. East, and A.G. Lee. 2005. The interfacial lipid binding site on the potassium channel KcsA is specific for anionic phospholipids. *Biophys.J.* 89:4081–4089.

Marius, P., M.R. de Planque, and P.T. Williamson. 2012. Probing the interaction of lipids with the non-annular binding sites of the potassium channel KcsA by magic-angle spinning NMR. *Biochim.Biophys.Acta*. 1818:90–96.

Marius, P., M. Zagnoni, M.E. Sandison, J.M. East, H. Morgan, and A.G. Lee. 2008. Binding of anionic lipids to at least three nonannular sites on the potassium channel KcsA is required for channel opening. *Biophys.J.* 94:1689–1698.

Marsh, D. 2008. Protein modulation of lipids, and vice-versa, in membranes. *Biochim.Biophys.Acta*. 1778:1545–1575.

McCormick, J.I., and R.M. Johnstone. 1988. Volume enlargement and recovery of Na+-dependent amino acid transport in proteoliposomes derived from Ehrlich ascites cell membranes. *J.Biol.Chem.* 263:8111–8119.

McCoy, J.G., and C.M. Nimigean. 2012. Structural correlates of selectivity and inactivation in potassium channels. *Biochim. Biophys. Acta - Biomembr.* 1818:272–285. doi:10.1016/j.bbamem.2011.09.007.

Meuser, D., H. Splitt, R. Wagner, and H. Schrempf. 1999. Exploring the open

pore of the potassium channel from Streptomyces lividans. *FEBS Lett.* 462:447–452.

Molina, M.L., F.N. Barrera, A.M. Fernández, J.A. Poveda, M.L. Renart, J.A. Encinar, G. Riquelme, and J.M. González-Ros. 2006. Clustering and coupled gating modulate the activity in KcsA, a potassium channel model. *J. Biol. Chem.* 281:18837–18848.

Molina, M.L., J.A. Encinar, F.N. Barrera, G. Fernandez-Ballester, G. Riquelme, and J.M. Gonzalez-Ros. 2004. Influence of C-terminal protein domains and protein-lipid interactions on tetramerization and stability of the potassium channel KcsA. *Biochemistry*. 43:14924–14931.

Molina, M.L., A.M. Giudici, J.A. Poveda, G. Fernández-Ballester, E. Montoya, M.L. Renart, A.M. Fernández, J.A. Encinar, G. Riquelme, A. Morales, and J.M. González-Ros. 2015. Competing lipid-protein and protein-protein interactions determine clustering and gating patterns in the potassium channel from streptomyces lividans (KcsA). *J. Biol. Chem.* 290:25745–25755. doi:10.1074/jbc.M115.669598.

Ostmeyer, J., S. Chakrapani, A.C. Pan, E. Perozo, and B. Roux. 2013. Recovery from slow inactivation in K+ channels is controlled by water molecules. *Nature*. 501:121–124.

Phillips, R., T. Ursell, P. Wiggins, and P. Sens. 2009. Emerging roles for lipids in shaping membrane-protein function. *Nature*. 459:379–385.

Poveda, J.A., A. Marcela Giudici, M. Lourdes Renart, A. Morales, and J.M. González-Ros. 2017. Towards understanding the molecular basis of ion channel modulation by lipids: Mechanistic models and current paradigms. *Biochim. Biophys. Acta - Biomembr.* 1859. doi:10.1016/j.bbamem.2017.04.003.

Poveda, J.A.A., A.M.M. Giudici, M.L.L. Renart, M.L.L. Molina, E. Montoya, A. Fernandez-Carvajal, G. Fernandez-Ballester, J.A.A. Encinar, J.M. Gonzalez-Ros, A. Fernández-Carvajal, G. Fernández-Ballester, J.A.A. Encinar, and J.M. González-Ros. 2014. Lipid modulation of ion channels

Formatted: English (U.S.)

Formatted: English (U.S.)

through specific binding sites. *Biochim.Biophys.Acta*. 1838:1560–1567. doi:10.1016/j.bbamem.2013.10.023.

Qin, F., A. Auerbach, and F. Sachs. 1996. Estimating single-channel kinetic parameters from idealized patch-clamp data containing missed events. *Biophys.J.* 70:264–280.

Qin, F., A. Auerbach, and F. Sachs. 1997. Maximum likelihood estimation of aggregated Markov processes. *Proc.Biol.Sci.* 264:375–383.

Raghuraman, H., S.M. Islam, S. Mukherjee, B. Roux, and E. Perozo. 2014. Dynamics transitions at the outer vestibule of the KcsA potassium channel during gating. *Proc.Natl.Acad.Sci.U.S.A*. 111:1831–1836.

Raja, M. 2010. The role of extramembranous cytoplasmic termini in assembly and stability of the tetrameric K(+)-channel KcsA. *J.Membr.Biol.* 235:51–61.

Raja, M., R.E. Spelbrink, K.B. de, and J.A. Killian. 2007. Phosphatidic acid plays a special role in stabilizing and folding of the tetrameric potassium channel KcsA. *FEBS Lett.* 581:5715–5722.

Riquelme, G., E. Lopez, L.M. Garcia-Segura, J.A. Ferragut, and J.M. Gonzalez-Ros. 1990. Giant liposomes: a model system in which to obtain patch-clamp recordings of ionic channels. *Biochemistry*. 29:11215–11222.

Rotem, D., A. Mason, and H. Bayley. 2010. Inactivation of the KcsA potassium channel explored with heterotetramers. *J.Gen.Physiol*. 135:29–42.

Roux, B., and R. Sauve. 1985. A general solution to the time interval omission problem applied to single channel analysis. *Biophys.J.* 48:149–158.

Sigworth, F.J., and S.M. Sine. 1987. Data transformations for improved display and fitting of single-channel dwell time histograms. *Biophys.J.* 52:1047–1054.

Triano, I., F.N.N. Barrera, M.L.L. Renart, M.L.L. Molina, G. Fernández-Ballester, J.A.A. Poveda, A.M. Fernández, J.A.A. Encinar, A.V. V Ferrer-Montiel, D. Otzen, J.M. González-Ros, G. Fernandez-Ballester, J.A.A. Poveda, A.M. Fernandez, J.A.A. Encinar, A.V. V Ferrer-Montiel, D. Otzen, and J.M.

Gonzalez-Ros. 2010. Occupancy of nonannular lipid binding sites on KcsA greatly increases the stability of the tetrameric protein. *Biochemistry*. 49:5397–5404. doi:10.1021/bi1003712.

Valiyaveetil, F.I., Y. Zhou, and R. MacKinnon. 2002. Lipids in the structure, folding, and function of the KcsA K+ channel. *Biochemistry*. 41:10771–10777.

Weingarth, M., E.A.W. Van Der Cruijsen, J. Ostmeyer, S. Lievestro, B. Roux, and M. Baldus. 2014. Quantitative analysis of the water occupancy around the selectivity filter of a K+ channel in different gating modes. *J. Am. Chem. Soc.* 136:2000–2007. doi:10.1021/ja411450y.

Weingarth, M., A. Prokofyev, E.A. van der Cruijsen, D. Nand, A.M. Bonvin, O. Pongs, and M. Baldus. 2013. Structural determinants of specific lipid binding to potassium channels. *J.Am.Chem.Soc.* 135:3983–3988.

Zhou, Y., J.H. Morais-Cabral, A. Kaufman, and R. MacKinnon. 2001. Chemistry of ion coordination and hydration revealed by a K+ channel-Fab complex at 2.0 A resolution. *Nature*. 414:43–48.

## TABLES

**Table 1**. Summary of simulations performed

| System | Bilayer Composition | Notation | Non-Annular Lipids? | Replica | Length (ns) |
|---|---|---|---|---|---|
| **WT** | PA/PC | WT-PA | N | 1 | 400 |
| | | | | 2 | 200 |
| | | WT-$PA_4$ | Y | 1 | 400 |
| | | | | 2 | 200 |
| | | | | 3 | 200 |
| | | | | 4 | 200 |
| | | | | 5 | 200 |
| | PC | WT-PC | N | 1 | 400 |
| | | | | 2 | 200 |
| | | WT-$PC_4$ | Y | 1 | 400 |
| | | | | 2 | 200 |
| | | | | 3 | 200 |
| | | | | 4 | 200 |
| | | | | 5 | 200 |
| **R64A** | PA/PC | R64A-PA | N | 1 | 200 |
| | | R64A-$PA_4$ | Y | 1 | 200 |
| | PC | R64A-PC | N | 1 | 200 |
| | | R64A-$PC_4$ | Y | 1 | 200 |
| **R64L** | PA/PC | R64L-PA | N | 1 | 200 |
| | | R64L-$PA_4$ | Y | 1 | 200 |
| | PC | R64L-PC | N | 1 | 200 |
| | | R64L-$PC_4$ | Y | 1 | 200 |
| **R89A** | PA/PC | R89A-PA | N | 1 | 200 |
| | | R89A-$PA_4$ | Y | 1 | 200 |
| | PC | R89A-PC | N | 1 | 200 |
| | | R89A-$PC_4$ | Y | 1 | 200 |
| **TOTAL Simulation Time** | | | | | 6 μs |

**Table 2**. Percentage of simulation time (considering only when ions are in S2/S4 or S1/S3 configurations (Figure S2)) where either one or both triad H-bond interactions (W67-D80 and E71-D80) are broken. A, B, C and D refers to each of the four monomers in the tetrameric channel.

| Simulation | S2/S4 or S1/S3 Configuration (ns) | H-Bond Disruption (%) | | | | | | | | | | | | | | |
|---|---|---|---|---|---|---|---|---|---|---|---|---|---|---|---|---|
| | | W67-D80 | | | | Avg. | E71-D80 | | | | Avg. | W67-D80 & E71-D80 | | | | Avg. |
| | | A | B | C | D | | A | B | C | D | | A | B | C | D | |
| R89A-PA | 59 | 1 | 66 | 60 | 90 | 54 | 0 | 49 | 47 | 89 | 46 | 0 | 49 | 46 | 89 | 46 |
| R89A-$PA_4$ | 90 | 31 | 96 | 68 | 20 | 54 | 19 | 96 | 61 | 8 | 46 | 18 | 96 | 61 | 7 | 46 |
| R89A-PC | 155 | 84 | 97 | 3 | 1 | 46 | 62 | 95 | 1 | 0 | 40 | 53 | 95 | 1 | 0 | 37 |
| R89A-$PC_4$ | 180 | 77 | 74 | 97 | 69 | 79 | 71 | 69 | 95 | 72 | 77 | 72 | 69 | 95 | 69 | 76 |
| R64A-PA | 200 | 1 | 1 | 1 | 3 | 2 | 0 | 0 | 0 | 0 | 0 | 0 | 0 | 0 | 0 | 0 |
| R64A-$PA_4$ | 200 | 2 | 0 | 1 | 2 | 1 | 0 | 0 | 0 | 2 | 0 | 0 | 0 | 0 | 0 | 0 |
| R64A-PC | 200 | 1 | 11 | 1 | 1 | 4 | 0 | 0 | 0 | 0 | 0 | 0 | 0 | 0 | 0 | 0 |
| R64A-$PC_4$ | 200 | 1 | 0 | 2 | 4 | 2 | 0 | 0 | 0 | 0 | 0 | 0 | 0 | 0 | 0 | 0 |
| R64L-PA | 48 | 0 | 1 | 0 | 1 | 1 | 0 | 0 | 0 | 0 | 0 | 0 | 0 | 0 | 0 | 0 |
| R64L-$PA_4$ | 200 | 1 | 5 | 10 | 1 | 4 | 0 | 3 | 0 | 0 | 1 | 0 | 2 | 0 | 0 | 0 |
| R64L-PC | 110 | 1 | 5 | 10 | 1 | 4 | 0 | 0 | 1 | 0 | 0 | 0 | 0 | 0 | 0 | 0 |
| R64L-$PC_4$ | 200 | 1 | 6 | 2 | 4 | 3 | 0 | 0 | 5 | 0 | 1 | 0 | 0 | 0 | 0 | 0 |
| $^{1}$WT-PA | 260 | 23 | 0 | 13 | 17 | 13 | 4 | 0 | 4 | 5 | 3 | 3 | 3 | 0 | 5 | 3 |
| $^{2}$WT-PA | 176 | 8 | 0 | 9 | 15 | 8 | 0 | 35 | 0 | 1 | 9 | 0 | 0 | 0 | 1 | 0 |
| $^{1}$WT-$PA_4$ | 200 | 3 | 3 | 33 | 2 | 10 | 0 | 1 | 8 | 0 | 2 | 0 | 0 | 8 | 0 | 2 |
| $^{2}$WT-$PA_4$ | 30 | 39 | 3 | 0 | 4 | 12 | 20 | 0 | 0 | 0 | 5 | 18 | 0 | 0 | 0 | 5 |
| $^{3}$WT-$PA_4$ | 200 | 9 | 2 | 4 | 1 | 4 | 0 | 0 | 0 | 28 | 7 | 0 | 0 | 0 | 0 | 0 |
| $^{4}$WT-$PA_4$ | 184 | 0 | 0 | 4 | 1 | 1 | 0 | 0 | 0 | 0 | 0 | 0 | 0 | 0 | 0 | 0 |
| $^{5}$WT-$PA_4$ | 200 | 1 | 12 | 5 | 7 | 6 | 0 | 3 | 0 | 2 | 1 | 0 | 2 | 0 | 1 | 1 |
| $^{1}$WT-PC | 102 | 1 | 3 | 0 | 3 | 2 | 0 | 0 | 0 | 0 | 0 | 0 | 0 | 0 | 0 | 0 |
| $^{2}$WT-PC | 165 | 31 | 1 | 50 | 0 | 21 | 14 | 0 | 44 | 0 | 15 | 13 | 0 | 44 | 0 | 14 |
| $^{1}$WT-$PC_4$ | 132 | 18 | 4 | 10 | 40 | 18 | 0 | 0 | 57 | 11 | 17 | 0 | 0 | 4 | 31 | 9 |
| $^{2}$WT-$PC_4$ | 133 | 1 | 29 | 4 | 0 | 9 | 0 | 27 | 0 | 0 | 7 | 0 | 27 | 0 | 0 | 7 |
| $^{3}$WT-$PC_4$ | 108 | 3 | 3 | 1 | 14 | 5 | 0 | 0 | 0 | 7 | 2 | 0 | 0 | 0 | 7 | 2 |
| $^{4}$WT-$PC_4$ | 43 | 9 | 0 | 2 | 5 | 4 | 0 | 0 | 0 | 0 | 0 | 0 | 0 | 0 | 0 | 0 |
| $^{5}$WT-$PC_4$ | 59 | 10 | 1 | 54 | 1 | 17 | 5 | 0 | 27 | 12 | 11 | 4 | 0 | 27 | 0 | 8 |

## FIGURE LEGENDS

**Figure 1. Schematic representation of the KcsA structure indicating potential binding regions for anionic lipids.** For the sake of clarity, only two out of the four KcsA subunits have been drawn. The location of important domains of KcsA such as the selectivity filter, the N- and C-terminus and the transmembrane segments TM1 and TM2 is indicated. Also, basic amino acid residues within the channel sequence reported as potential sites for anionic lipid binding are depicted like spheres: N-terminal R11 and K14 residues (in violet); R27, R117, R121 and R122 residues (in yellow), situated at the cytoplasmic side close to the C-terminal; and those present at the non-annular lipid binding sites, R64 and R89 (in red).

**Figure 2. Macroscopic inactivation of KcsA.** Normalized macroscopic currents elicited by pH jumps (pH 7 to 4) are shown. Each trace is the average from three to five different experiments. (A) Influence of anionic phospholipid on KcsA inactivation. $K^+$ currents were recorded from macropatches of WT KcsA reconstituted in plain asolectin lipids (WT), asolectin lipids with an added 25% of egg PA (WT+25%PA) or asolectin lipids with an added 50% of egg PA (WT+50%PA). (B) Effects of R64A, R89A and R64,89A KcsA mutations on channel inactivation upon reconstitution of the arginine mutant channels in plain asolectin lipids. (C) Effects of adding 25% PA to the reconstituted asolectin lipid matrix of the arginine mutants mentioned above. The holding potential in all these experiments was +150 mV.

**Figure 3. Effect of the anionic phospholipid lipid PA on WT KcsA single channel currents.** Panel A shows a long, representative recording taken at +150 mV from a membrane patch containing WT KcsA reconstituted in plain asolectin lipids. The recording serves to illustrate heterogeneous bursts of channel activity with different amplitudes throughout. Out of that heterogeneity, panel B shows in more detail shorter recordings of the different currents at +150 and -150 mV found for the WT channel reconstituted in plain asolectin lipids (upper traces) or in asolectin supplemented with 25% (mid traces) or 50% (lower traces) PA. The asterisks indicate the prevalent, most frequently found current in each experimental condition. Panel C shows the amplitude

histograms for the open state currents found under the different reconstitution conditions from above and illustrates that the amplitude of the most frequently found currents increases as the percentage of added PA is increased. Notice that the analysis of data used for the histograms to illustrate the distribution of open states, do not include the long silent periods in the recordings and therefore, the relative importance of the open state population is overestimated. The histograms shown are the summation of 9 to 15 individual histograms from different samples.

**Figure 4. I/V curves of WT KcsA single channel currents.** The figure shows the I/V curves for the most frequently found currents under the different reconstitution conditions specified in Figure 3. In addition to the already mentioned increase in current amplitude caused by the added PA, the figure shows that the rectification seen in plain asolectin remains regardless of the added PA content. Data points and error bars are the average and s.e.m. of 10 to15 different samples.

**Figure 5. Effects of added PA on single channel currents from arginine to alanine mutants of KcsA reconstituted in asolectin lipids.** Only the most frequently found, prevalent current from the recordings of each of the mutants at +150 and -150 mV are included in the figure. Compared to the WT channel in plain asolectin in Figure 3B, all arginine to alanine mutants exhibit much higher open probabilities and higher amplitudes. Also, in contrast to the WT channel, addition of 25 or 50% PA to the reconstituted bilayers results in little (only in the R64A-KcsA mutant at positive voltages) or no effects on further increasing the current amplitudes. Moreover, I/V curves to the right in each panel show an essentially ohmic behavior for all three mutants. Symbols used in this Figure are as in Figure 4. Data points and error bars are the average and s.e.m. of 10 to 15 different samples.

**Figure 6. Kinetic behaviour of KcsA is modulated by PA and non-annular arginine mutations.** (A) Representative dwell time distribution of closed and open events within bursts identified using $t_{crit}$, (see Methods section). The solid line denotes the density function calculated by fitting the data to two closed and one open state model (see text). (B) Kinetic parameters

derived from the above fitting. $k_f$ and $k_i$ refer to the flickering and intermediate closing rate constants, respectively (see text). Data are the mean values ± s.e.m. of 4 to 7 different samples.

**Figure 7. Salient features of R64L-KcsA mutant $K^+$ currents**. Panel A shows normalized macroscopic currents at a holding potential of +150 mV from fast pH jumps (pH 7 to 4) in macropatches containing the mutant channel reconstituted in plain asolectin lipids with or without added PA. The behavior of the wild-type KcsA channel reconstituted in plain asolectin under comparable experimental conditions, has been added for comparison. Each trace is the average from three different experiments. Panel B shows representative single channel recordings at +150 and -150 mV of the prevalent current from this mutant channel reconstituted in plain asolectin with or without added PA.

**Figure 8. Solution NMR spectroscopy**. Guanidino region of the $^{1}H,^{15}N$-HSQC spectra of detergent-solubilized wild-type KcsA in the absence of any ligand (blue contours) and in the presence of PA (green contours) or PC (red contours) at protein to lipid molar ratios of 1:3 and 1:5, respectively. A) Overlay of KcsA channel with and without PA. B) Overlay of KcsA channel with and without PC. The assigned residues are indicated in black arrows.

**Figure 9. MD simulations of WT KcsA.** (A) D80-R89 interaction frequency in WT-KcsA simulations. (B) Average number of lipid H-bonds in WT-KcsA simulations, calculated using a 3.5 Å distance cutoff between polar atoms and $35^{o}$ cutoff for the acceptor-donor-hydrogen angle. (C) Dominant H-bond configuration of non-annular PA, which disrupts D80-R89 interactions. (D) Example of a H-bond scenario where D80 and R89 interact in spite of bound PC. For (C-D) the simulation and subunit shown is marked with an asterisk in (A-B). Data for the remaining simulations can be found in Figure S1.

**Figure 10. MD simulations of R64A and R64L mutant channels.** (A) D80-R89 hydrogen bond frequency in R64A-KcsA and R64L-KcsA simulations. (B) Depiction of opposing scenarios in R64A (grey sidechains) and R64L (orange sidechains) mutant channels. The specific simulation and subunit shown is marked with an asterisk in (A).